Surface Clutter Suppression Techniques Applied to P-band Multi-Channel SAR Ice Sounder Data from East Antarctica

Lin, Chung-Chi; Bekaert, David ; Gebert, Nicolas ; Heliere, Florence; Buck, Christopher; Casal, Tania; Davidson, Malcolm; Dall, Jørgen; Kusk, Anders; Kristensen, Steen Savstrup

Publication date:
2012

Document Version
Publisher's PDF, also known as Version of record

Surface Clutter Suppression Techniques Applied to P-band Multi-Channel SAR Ice Sounder Data from East Antarctica

Chung-Chi Lin[1], David Bekaert[1], Nicolas Gebert[1], Florence Hélière[1], Christopher Buck[1], Tania Casal[1], Malcolm Davidson[1], Jørgen Dall[2], Anders Kusk[2], Steen Savstrup Kristensen[2], Juan Mosig[3] and Jean-François Zürcher[3]

[1]*European Space Agency, ESTEC, Noordwijk, The Netherlands; Chung-Chi.Lin@esa.int*
[2]*Technical Univ. Denmark, National Space Institute, Lyngby, Denmark; jd@space.dtu.dk*
[3]*Swiss Fed. Institute of Tech., Lab. Electromagnetics and Acoustics, Lausanne, Switzerland; Juan.Mosig@epfl.ch*

Abstract. Radar ice sounding allows for the retrieval of ice depth and provides information on basal topography, basal conditions, flow, and layering. In the prospect of a possible future satellite ice sounding mission, surface clutters are expected to severely hamper measurement of radar echoes from the depth due to the unfavourable observation geometry. Synthetic aperture radar (SAR) processing enables to attenuate surface clutters in the forward and backward directions, but not in the across-track directions. Thus, additional across-track clutter cancellation is a crucial step for extracting weaker subsurface radar echoes. ESA's P-band POLarimetric Airborne Radar Ice Sounder (POLARIS), recently upgraded with a larger antenna of 4 m length, enables simultaneous reception of up to 4 sub-aperture channels in across-track. Laboratory of Electromagnetics and Acoustics of Swiss Fed. Institute of Tech., Lausanne, developed and built the radiator-elements of the enhanced POLARIS. Several datasets were acquired in the multi-channel configuration during the Feb. 2011 campaign over East Antarctica. The POLARIS instrument will be briefly introduced, followed by an overview of the sounding campaign. Finally, different surface clutter suppression approaches, based on topographic data, are presented and compared. Clutter rejection performance is quantified through comparison with original data.

Keywords. Radio echo sounding, ice sheet, Antarctica, surface clutter suppression, multi-channel processing.

1. Introduction

1.1. Radar Ice Sounding from Space:

Understanding the role of the cryosphere in the climate change is one of the key elements of ESA's Living Planet programme [1]. Radar ice sounding, with its capability to provide three-dimensional characteristics of the major ice-sheets, represents a very important tool, as this will improve the understanding of their history and possible future evolution through the climate change. Global coverage and observations of uniform quality call for a spaceborne sensor. Such satellite-based sounding mission ideas have been proposed to ESA in the frame of "Call for Ideas for Earth Explorer Core and Opportunity Missions" (see e.g. [2]). Attenuation in ice of electromagnetic waves increases with increasing frequency. It is for this reason that current airborne sensors for ice sounding operate at low frequencies, e.g. 60 or 150 MHz [3][4], allowing imaging of the bed-rock underneath. Unfortunately, such low frequencies require antenna dimensions that cannot be easily accommodated in a launcher, thereby imposing a higher frequency to compensate for limited antenna size. The lowest frequency range allocated by ITU regulations to active sensing from space is from 432 to 438 MHz (P-band). P-band potentially represents a good compromise between the necessary antenna dimensions for achieving a required gain and penetration capability of the radar waves through ice sheets. Nevertheless, at P-band, the surface clutter masking the subsurface echoes represents a major obsta-

cle when operated from an Earth-orbiting satellite at altitude of several hundred kilometres [5], asking for sophisticated signal processing approaches to suppress clutter [6].

1.2. POLARIS:

In order to assess the capability of a hypothetical satellite-borne ice sounding mission, ESA's airborne POLARIS instrument [7], developed by the Tech. Univ. Denmark, operates at P-band in a nadir-pointing geometry. POLARIS was first deployed over Greenland in 2008 [8] and later in 2009 in a single aperture, dual and polarimetric configurations. The 2009 campaign included over-flights above the NEEM and NGRIP ice core drill-sites in the directions parallel and orthogonal to the ice flow for studying the effects of the bi-refringence. Results of those campaigns demonstrated the high sensitivity of POLARIS, capable of imaging the bedrock at 3000 m depth (see Figure 1).

Subsequently, POLARIS was enhanced with a larger antenna of 4 m length, having eight radiators grouped into four independent phase centers, enabling simultaneous reception, digitization and storage of up to 4 channels. This allows for digital beam-form processing, i.e. weighting and coherent combination of these channels. The upgraded POLARIS, for which the key parameters are summarized in Table 1, was flown over Antarctica in Feb. 2011.

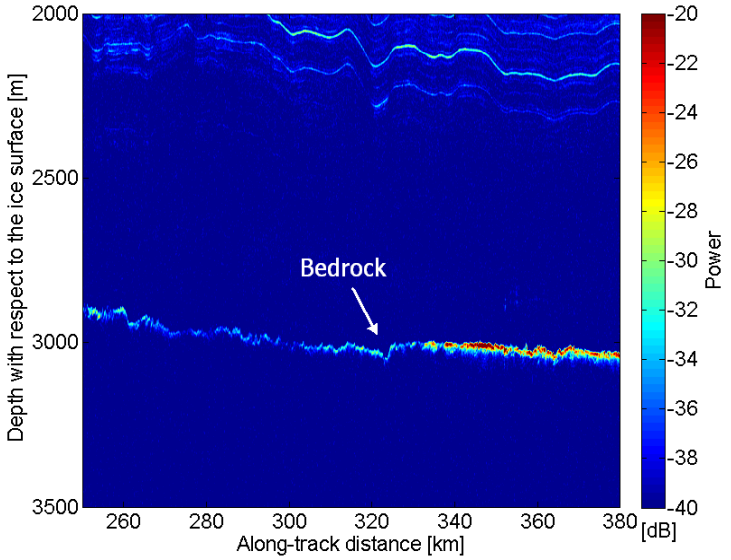

Figure 1: POLARIS ice sounding result Greenland.

Table 1: Key parameters of POLARIS.

Parameter	**Value**
Centre frequency	435 MHz
Wavelength in air	0.69 m
Transmitted bandwidths	85/30/6 MHz
Number of channels	4
Number of elements	8
Element spacing (wrt. centre)	0.48 m
Element length	0.408 m

2. Surface Clutter Suppression Techniques

Surface echoes exhibiting the same delay time as the sounding echo from a given depth are referred to as surface clutter. In case of a nadir-looking sensor and when assuming flat topography for a synthetic aperture system, where along-track ambiguities are suppressed by Doppler processing, this would result in two ambiguous across-track surface returns from symmetric angles with respect to the nadir. Accounting for the airplane roll, as well as topographic variations, makes the situation more complex, as the clutter returns will no longer be symmetric about nadir and even more than two surface clutter cells are possible. Figure 2 illustrates such an example at a given instant in time, highlighting for a specific depth R_{ice} the ambiguous angles θ_c^i where surface clutter is originating from. The angles θ_c^i are not stationary but evolve with time during the echo reception.

The basic idea is to make use of some multiple phase-center processing steps aiming at the suppression of the surface clutter. Different processing approaches, all based on the coherent weighting and combination of the individually received signals, will be reviewed in this section.

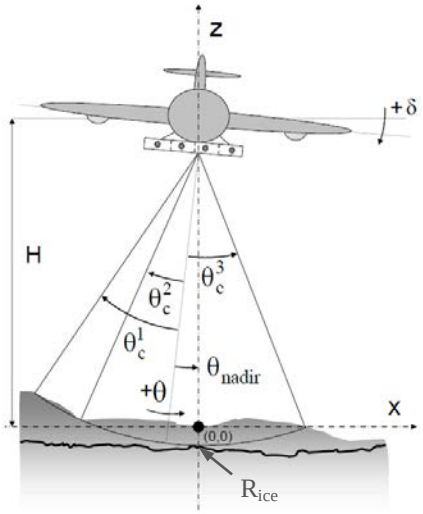

Figure 2: Illustration of clutter cancellation geometry.

2.1. Optimum Beam-former

With a simple beam-steering approach, a phase slope is applied across the individual channels, such that the receive gain of the antenna is maximum toward a pre-defined angle, e.g. θ_{nadir}, shown as 0° in Figure 3. With beam-steering, one maximizes the desired signal power and thus the signal-to-(thermal) noise ratio (SNR) toward the sounding direction, but does not account for the clutter [9]. A more sophisticated approach is offered by the application of a time-dependent null-steering: the complex weights of the individual channels in the coherent summation are chosen such that nulls in the synthesized receive antenna pattern are generated toward the expected clutter directions. A system with N channels allows for the steering of N-1 nulls [9]. Calculation of the weighting coefficients for the beam synthesis is based on the covariance matrix of the 'coloured' noise, represented by the surface clutter from specific directions. This means that this approach is optimum in terms of maximizing the clutter suppression, it might however degrade the SNR as it is based on a network of inverse filters. An example is provided in Figure 4 where nulls are generated at -45, 20 and 50°, however a low antenna gain is achieved toward the nadir.

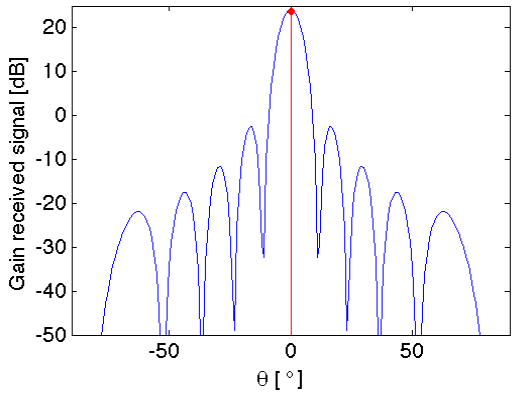

Figure 3: Receive antenna gain for beam-steering

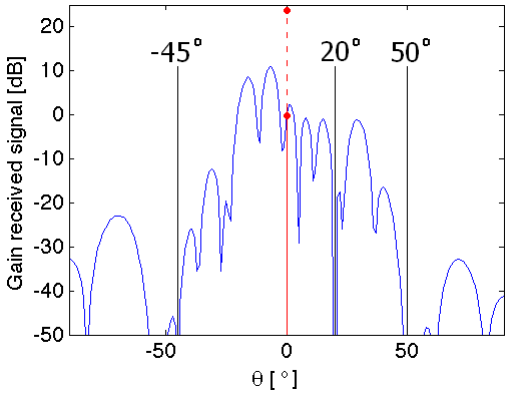

Figure 4: Receive antenna gain for null-steering (with 3 clutter sources at -45, 20 and 50°).

An optimum solution, where the clutter signals are minimized and where at the same time the echo from the depth (i.e. nadir) is being maximized, is then given by the combination of the two techniques described above. Regarding the derivation of the weighting coefficients, one can observe that the covariance matrix is based on the coloured noise, but will additionally be loaded with the white noise components. Practically, the weights w can then be calculated by inverting the noise covariance matrix R as given by [9] as:

$$w = R^{-1} s_{nadir}$$

$$R = \sigma_n^2 \mathrm{I} + \sum_{i=1}^{m} \sigma_i^2 \, s_i s_i^T$$

such that the sum of noise (σ_n^2) and the clutter power (σ_i^2) of the i directions is minimised and subjected to a unitary gain constraint, ensuring constant gain in the direction of interest, i.e. $w \cdot s_{nadir} = 1$. s_{nadir} is the steering vector in the direction of interest (nadir) and R the weighted sum of the identity matrix (representing white noise) and the matrices evolving from the steering vectors in the directions of the surface clutters s_i. The power ratio σ_i^2 / σ_n^2 between the clutter and the respective noise contributions is denoted as the Clutter-to-Noise Ratio (CNR).

Based on the above approach, a processing tool has been developed for clutter suppression, which uses the ice topography and platform roll angle to compute the angular position of the clutter sources. The latter could also be directly estimated from the data them-selves using a direction-of-arrival estimation technique as demonstrated e.g. in [10].

As 4 independent receive channels are available, clutter echoes can theoretically be suppressed in up to three pre-selected directions simultaneously. In practice, the number of suppressed directions should be subject to a trade-off, as will be demonstrated in the following. E.g. in the presence of strong surface clutter echoes from 3 different angular directions, the optimum strategy might be to suppress all 3 echoes, at the expense of increased thermal noise. Thus, the processor will be extended such that the local incidence angle, which strongly influences the backscattered power, will be considered. More specifically, topographic information will be used to derive an estimate of the local incident angle and additionally consider this parameter to determine the strongest echoes from up to 3 different angular directions.

Alternatively, another possible strategy would aim at suppression of clutter from only 2 directions and would benefit from the third degree of freedom in order to improve the thermal SNR. Figure 5 shows an example of optimum beam-forming where nulls are generated at -40 and 50° and at the same time the gain towards nadir is maximized.

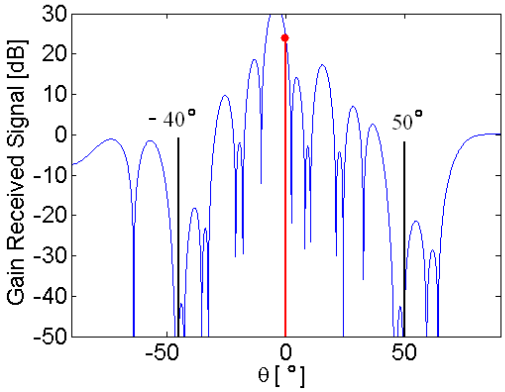

Figure 5: Synthesised receive antenna gain for optimum beam-forming (with 2 clutter sources at -40 and 50°).

2.2. Performance/Sensitivity Analysis

In this section, a sensitivity analysis is presented by comparing the receive signal gain after applying the optimum beam-former, i.e. taking into account the coherent weighting of the channels. All simulations assumed a flight with no roll at an altitude of 600 m and flat topography, resulting in two clutter sources, symmetric about nadir. The additional clutter angle is manually introduced at 60°. The maximum gain level in the antenna pattern is obtained when only beam-steering is applied. This corresponds to the case where thermal noise dominates over the clutter noise, being equivalent

to CNR = -∞ (in 10×log scale). When stronger clutter echoes are present, CNR increases and the weights are computed accordingly. One could for example put higher weight on clutter suppression. Note however that the combination of the transmit antenna pattern and that of a single receiver channel already attenuates the clutter, resulting in a CNR decreasing with increasing incidence angle, denoted as CNR(θ). As a result, there is no need to put high weight on clutter suppression, thereby allowing to maintain high receive gain in the direction of interest.

Figure 6 shows the result of sensitivity analysis of the normalized gain versus ice depth, comparing theoretical performance among the beam-steering technique (BS), optimized for SNR, the null-steering (NS) technique (CNR=100 dB), optimized for signal-to-clutter ratio SCR, and the optimum beam-former (OBF) approach (CNR(θ) = f(θ)·40 dB), optimized for the combination of both SCR and SNR. Moreover, a comparison is made between cases with 2 and 3 clutter sources. The normalized gain in nadir direction, Figure 6a, represents the signal power, while the normalized summed gain in the ambiguous directions, Figure 6b and 6c, represents the clutter power. Thermal noise is white and thus is not affected by the processing.

Regarding the signal power, one can conclude that null-steering alone (green dashed line) results in a loss of signal power, as it only aims at steering nulls to the clutter directions. Note that this is not realistic, as it assumes absence of thermal noise, but was chosen to demonstrate the inverse character of the weighting functions, which lead to a strong degradation of signal power (and thus SNR). Moreover, one can observe the grating lobe at around 210 m depth, resulting in a singularity. Using a more realistic value for the CNR, e.g. CNR(θ) = f(θ)·40 dB, results in a reduced but still considerable loss of signal power of 2.5-3 dB (dashed blue line). A clear improvement is obtained when suppressing only two directions. This leads to an extra degree of freedom that can be used to steer the main lobe thereby increasing the signal power of the optimum beam-former (blue solid line) to the level of the optimum beam-steering case (red solid line).

Regarding the clutter power, the worst case is represented by the beam-steering, which does not include any suppression of clutter echoes. As a result, the clutter power is directly determined by the combined antenna pattern, i.e. the full antenna aperture on transmit and a single channel on receive (Figure 6b and 6c, solid and dashed red lines). In contrast, applying the optimum beam-former results in a clear reduction of clutter power, as can be seen from the solid and dashed blue lines. In particular for strong clutter echoes at low depths, the clutter is clearly suppressed compared to the beam-steering case (red lines). Finally for the sake of completeness, consider the unrealistic case which assumes absence of thermal noise. As expected, this case exhibits excellent clutter suppression below -200 dB (Figure 6c, dashed green line).

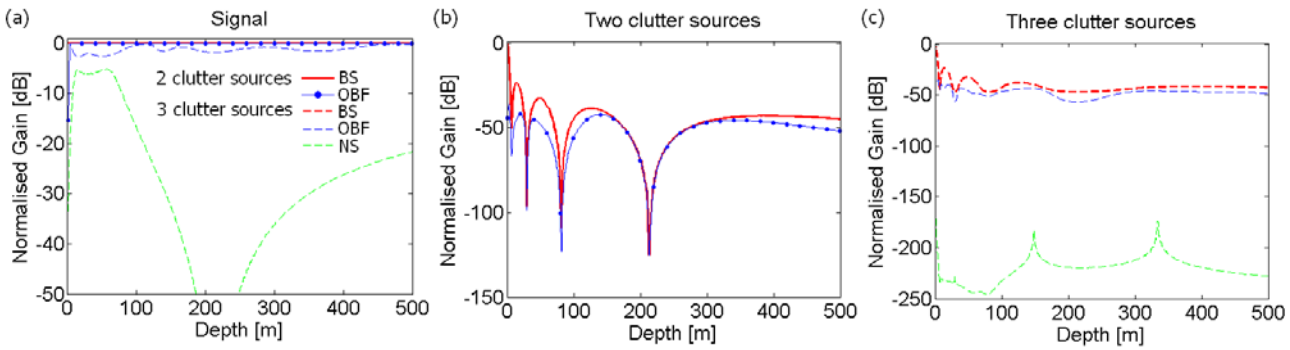

Figure 6: Result of sensitivity analysis of the normalized signal gain (a) and the normalized summed clutter gain, assuming beam-steering, null-steering and the optimum beamformer, for 2 (b) and 3 (c) clutter sources.

3. Application to POLARIS Campaign Data

3.1. POLARIS Campaign in East Antarctica

The POLARIS Antarctic campaign was conducted in Feb. 2011 in combination with the IceGrav 2011 campaign. The IceGrav project is a close scientific collaboration between Tech. Univ. Denmark, Nat. Geospatial-Intel. Agency, Univ. of Texas, Univ. of Bergen/NPI/Norway, IAA/Argentina and Brit. Antarctic Survey/UK. The primary goal is to measure airborne gravity in hitherto unmapped areas, and eventually contribute to a coordinated Antarctic gravity grid compilation, for basic use in geodesy, geophysics, and satellite orbit determination. The secondary goal is to provide basic radar, laser and magnetic data, as made possible by the rather large long-range DC-3 aircraft. Specifically for the Antarctic campaign, POLARIS was airworthiness-certified for the Basler DC-3 of Ken Borek Air Ltd. Figure 7 depicts the DC-3 aircraft with the POLARIS antenna mounted under the fuselage behind the wings. Also seen is the dipole antenna of the 60 MHz radar sounder mounted under the left wing, whereas another one is mounted under the right wing.

Figure 8 shows the POLARIS costal flight tracks ending over the Jutulstraumen glacier in the center of the map (KM9a to KM10) where the 4-channel multi-phase-center acquisitions were carried out. In this mode, POLARIS operated in single linear polarization which was orthogonal to the flight direction. The polarization can be switched by changing the internal cabling within the antenna housing.

Figure 7: Basler DC-3 with the POLARIS antenna mounted under the fuselage

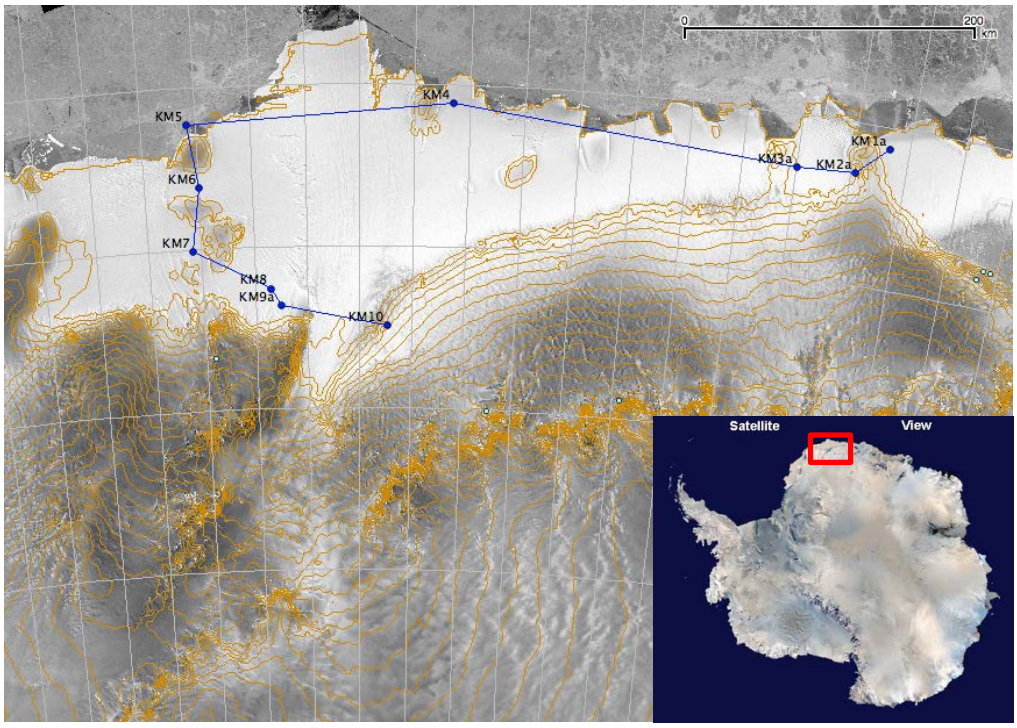

Figure 8: POLARIS coastal flight tracks over the campaign area in East Antarctica – starting from KM1a and ending at KM10 over the Jutulstraumen glacier (the inset shows the campaign area marked with red rectangle).

3.2. Processing Results

Two flight tracks, one across and the other along the ice flow as depicted in Figure 9, were selected for illustrating the multi-phase-center processing. A high flight altitude of 3250 m was chosen in order to approximate the satellite observation geometry. A flat ice surface was assumed for the processing as no laser topography data were yet made available at the time of the analysis.

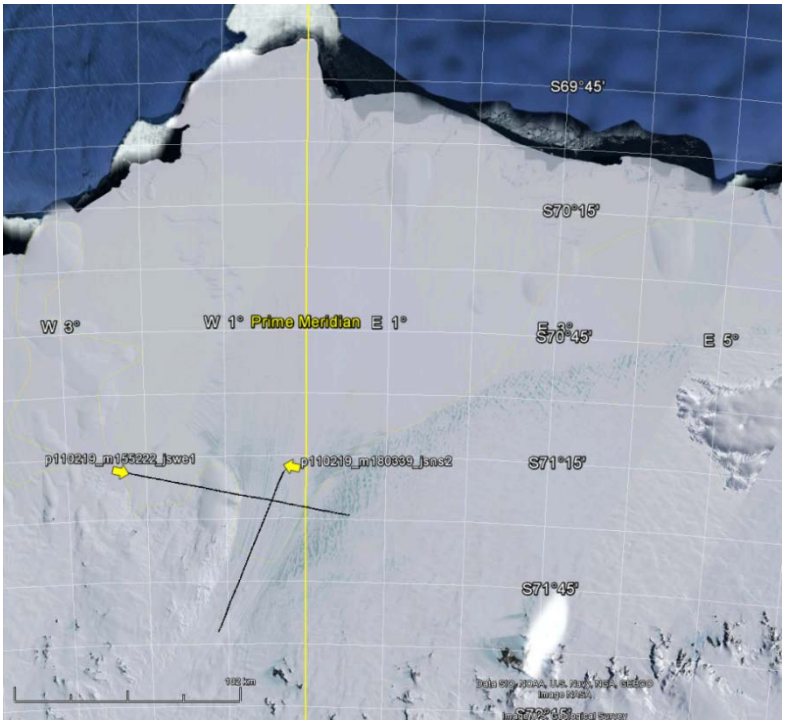

Figure 9: Two POLARIS flight tracks over the Jutulstraumen glacier: the across-flow track from left to right (West to East); and the along-flow track from North to South (down- to up-stream).

Figure 10 shows the comparison of the across-flow ice profile without (left) and with (right) the multi-phase-center processing. The red vertical line indicates the crossing position with respect to the along-flow flight track. The glacier flow is seen on the right-hand half of the profile from about 55 to 90 km along-track

distance. Comparing the two figures, one can notice a substantial reduction of the reflectivity (~10 dB) in the depth zone of 300 to 450 m. A detailed analysis of the reflectivity profile reveals some improvement down to the depth of 700 m. For larger depths, no significant difference can be observed. The average reflectivity scale is also different between the two figures as the optimum beam-forming reduces the system gain at the cost of generating time-dependent nulls in appropriate directions.

Figure 11 shows the comparison of the along-flow sounding profile from the down- to up-stream direction without (left) and with (right) the multi-phase-center processing. The red vertical line indicate the crossing position with respect to the across-flow flight track. One can clearly see the thinning of the ice along the flow (right to left), i.e. it is discharging onto the sea water. The hydrostatic equilibrium is reached where the surface slope becomes null. Similar to the previous case, one can clearly see a substantial reduction of the reflectivity in the depth zone of 200 to 350 m from the surface, with some minor improvement extending to around 600 m from the surface.

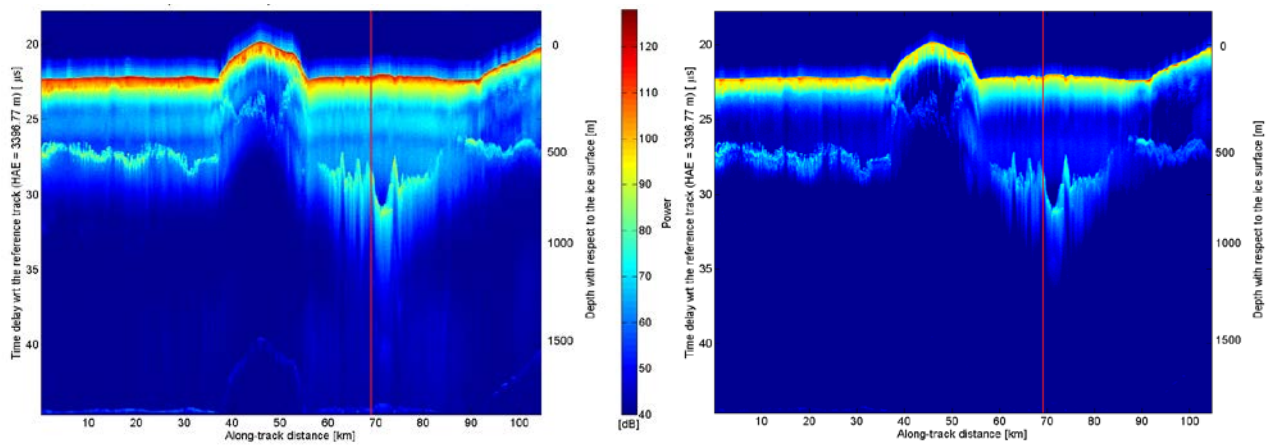

Figure 10: Across-flow sounding profile of the Jutulstraumen glacier (West to East) – without (left) and with (right) multi-phase-centre processing.

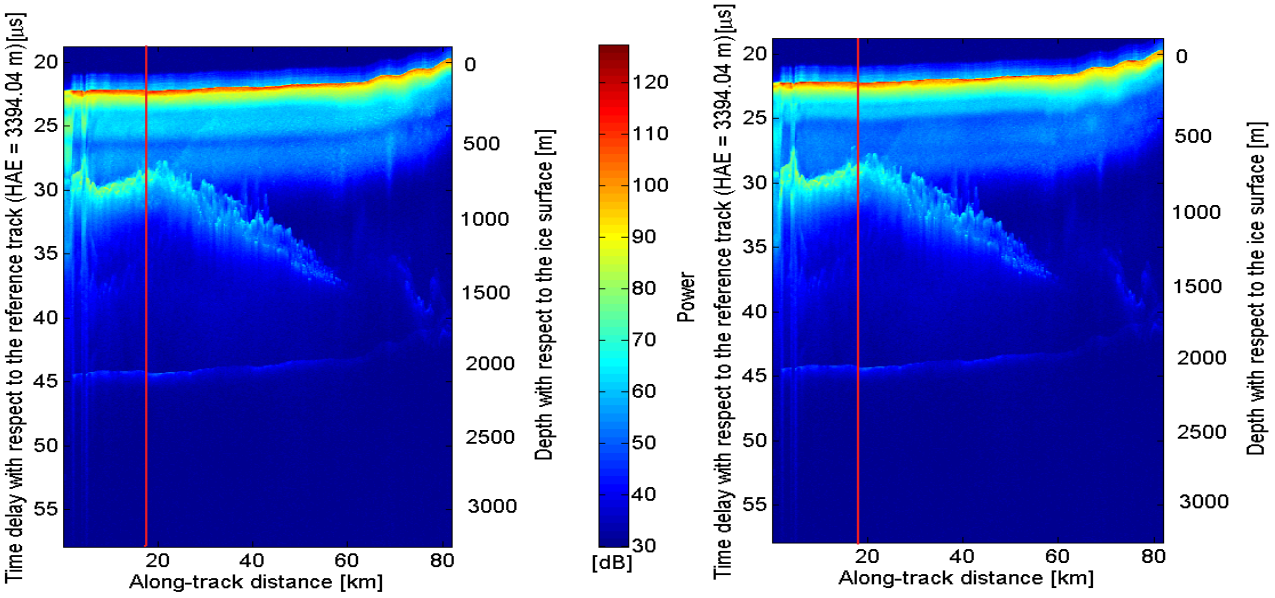

Figure 11: Along-flow sounding profile of the Jutulstraumen glacier (from down- to up-stream) – without (left) and with (right) the multi-phase centre processing.

4. Conclusion

The multi-phase-center capability of POLARIS was tested for the first time over the Jutulstraumen glacier in Feb. 2011. An optimum beam-former processing for POLARIS was developed and used to validate its enhanced functionality and technique for clutter suppression. The optimum beam-former minimizes the weighted sum of the instrument thermal noise and clutter power, and at the same time maximizing the sounding echoes from the depth for a pre-determined direction. A successful application of the technique has been demonstrated with an attenuation of the off-nadir clutter power of up to 10 dB. The optimum beam-forming algorithm is sensitive to the surface scattering model used to estimate the clutter power, as its relative importance with respect to the instrument thermal noise must be known a priori. Thus, a realistic assumption on its incidence angle dependence is needed which is mainly related to the ice surface roughness.

Acknowledgements

The authors would like to thank Dr. René Forsberg of Tech. Univ. Denmark, Mr. Hugh Corr of British Antarctic Survey and Dr. Kenichi Matsuoka of Norwegian Polar Institute for their valuable advises on the selection of POLARIS campaign sites and logistic supports on sites.

References

[1] *The Changing Earth*. ESA Publication SP-1304, July 2006, available on-line at http://www.esa.int/esaLP/ASERBVNW9SC_index_0.html

[2] Hérique A, W. Kofman, P. Baüer, F. Rémy, L. Phalippou, 1999. *A Spaceborne Ground Penetrating Radar: MIMOSA*. Proc. CEOS Workshop on SAR Calibration and Validation, ESA Publication SP-450, Toulouse, France, Oct. 1999.

[3] Peters M, D. Blankenship, S. Carter, S. Kempf, D. Young, and J. Holt, 2007. *Along-Track Focusing of Airborne Radar Sounding Data From West Antarctica for Improving Basal Reflection Analysis and Layer Detection*. IEEE Trans. Geosc. & Rem. Sens. vol. 45 (9), Sep. 2007, pp. 2725-2736.

[4] Hélière F, C.C. Lin, D. Vaughan and H. Corr, 2007. *Radio Echo Sounding of Pine Island Glacier, West Antarctica - Aperture Synthesis Processing and Analysis of Feasibility from Space*, 2007. IEEE Trans. Geosc. & Remote Sensing, Vol. 45, Aug. 2007, pp2573-2582.

[5] Jezek K.C, S. Gogineni, X. Wu, E. Rodriguez, F. Rodriguez-Morales, A. Hoch, A. Freeman, J.G. Sonntag, 2011. *Two-Frequency Radar Experiments for Sounding Glacier Ice and Mapping the Topography of the Glacier Bed*. IEEE Trans. Geosc. & Rem. Sens. vol. 49 (3), March 2011, pp.920-929.

[6] Scheiber R, P. Prats, F. Hélière, 2008. *Surface Clutter Suppression Techniques for Ice Sounding Radars: Analysis of Airborne Data*. Proc. of EUSAR, Friedrichshafen, Germany, June 2008.

[7] Dall J, S.S. Kristensen, V. Krozer, C.C. Hernández, J. Vidkjær, A. Kusk, J. Balling, N. Skou, S.S. Søbjærg, E.L. Christensen, 2010. *ESA's polarimetric airborne radar ice sounder (POLARIS): Design and first results.* IET Radar, Sonar & Navigation, vol. 4 (3), 2010.

[8] Villano M, F. Hélière, C.C. Lin, P. Fabry, A. Kusk, 2009. *Synthetic Aperture Processing of Ice Sounding Radar Data: Results from POLARIS Test Campaign*. 2nd Workshop on Advanced RF Sensors and Remote Sensing Instruments, 16-18 Nov. 2009, Noordwijk, The Netherlands.

[9] Guerci J.R, 2003. *Space-Time Adaptive Processing* (Artech House).

[10] Nielsen U, J. Dall, S. S. Kristensen, A & Kusk, 2012. *Coherent Surface Clutter Suppression Techniques with Topography Estimation for Multi-Phase-Center Radar Ice Sounding*. EUSAR 2012 Conference Proceedings, Nuernberg, Germany, April 2012.